

Implicit Incorporation of Heuristics in MPC-Based Control of a Hydrogen Plant

Thomas Schmitt¹, Jens Engel¹, Martin Kopp², Tobias Rodemann¹

Abstract—The replacement of fossil fuels in combination with an increasing share of renewable energy sources leads to an increased focus on decentralized microgrids. One option is the local production of green hydrogen in combination with fuel cell vehicles (FCVs). In this paper, we develop a control strategy based on Model Predictive Control (MPC) for an energy management system (EMS) of a hydrogen plant, which is currently under installation in Offenbach, Germany. The plant includes an electrolyzer, a compressor, a low pressure storage tank, and six medium pressure storage tanks with complex heuristic physical coupling during the filling and extraction of hydrogen. Since these heuristics are too complex to be incorporated into the optimal control problem (OCP) explicitly, we propose a novel approach to do so implicitly. First, the MPC is executed without considering them. Then, the so-called allocator uses a heuristic model (of arbitrary complexity) to verify whether the MPC’s plan is valid. If not, it introduces additional constraints to the MPC’s OCP to implicitly respect the tanks’ pressure levels. The MPC is executed again and the new plan is applied to the plant. Simulation results with real-world measurement data of the facility’s energy management and realistic fueling scenarios show its advantages over rule-based control.

Index Terms—Convex optimization, mixed integer programming, hydrogen pressure, hydrogen refueling station, energy management

I. INTRODUCTION

A. Motivation

The push for decarbonization of the global economy has spurred an increasing adoption of renewable energy sources like wind and solar power. However, the variability of these sources poses challenges for integration into the centralized public power grid. Therefore, local microgrids will become more important to support the decentralization of the power grid. Hydrogen emerges as a compelling solution for long-term energy storage due to its high energy density and the possibility of emission-free production. In addition, fossil fuels will have to be replaced in the transportation sector. While battery electric vehicles are likely to represent the bulk of the private transportation sector, the number fuel cell vehicles (FCVs) is expected to increase, too, with different projections from 582,000 units in 2030 worldwide [1] up to over 10,000,000 [2]. In combination with the above mentioned decentralization, this necessitates the intelligent production and storage of hydrogen, possibly in form of local energy management systems (EMSs).

¹Honda Research Institute Europe GmbH, Offenbach, Germany. E-mail: {thomas.schmitt, jens.engel, tobias.rodemann}@honda-ri.de

²Honda R&D Europe (Deutschland) GmbH, Offenbach, Germany. E-mail: martin_kopp@de.hrdeu.com

Funded by HA Hessen Agentur GmbH

As part of a research project, Honda Europe R&D (Deutschland) GmbH is currently installing a hydrogen production system including a hydrogen refueling station (HRS) in Offenbach, Germany. It will be connected to the currently existing energy infrastructure [3] and consists of an electrolyzer, a compressor, a low pressure (LP) storage tank and six medium pressure (MP) storage tanks. The MP tanks are divided into two sections, and their physical coupling during the filling and removal of hydrogen follows complex rules. In this paper, we present an approach on how an EMS based on Model Predictive Control (MPC) can be developed for the planned system despite its complexity.

B. Literature Review

MPC is regularly being considered for hydrogen systems. However, while many works extensively consider the modeling of the hydrogen production part, e. g. the electrolyzer’s efficiency curve or security constraints [4], the hydrogen’s pressure when stored is usually neglected. In [5], MPC is used for an on-site HRS which is set to be built in Zaragoza, Spain. The plant consists of multiple electrolyzers, compressors and storage tanks and should serve both light duty vehicles (700 bar) and heavy duty vehicles (350 bar). While it has 3 cascaded tanks to serve the dispenser of the heavy duty vehicles with a maximum of 500 bar, the MPC does not respect the actual pressure levels of the tanks. Namely, neither the mass flow rates vary, nor is there a distinction if the tank pressure is high enough to refill the vehicle completely. In [6], a two-layered MPC strategy is developed to control a wind-powered hydrogen-based microgrid. The higher level MPC schedules the hydrogen production of an electrolyzer for a time horizon of 24 h while respecting the demand from FCVs and possible grid loads. The lower level MPC is then supposed to track the production setpoints in real-time with a time horizon of 1 h, while additionally respecting the electrolyzer’s status (warm vs. cold) in form of an automaton. However, the hydrogen storage’s pressure is neglected completely. This neglect in combination with MPC is most likely due to the complexity of modeling the fueling process with all relevant parameters, e. g. temperature and pressure. Usually, these processes are modeled with modeling languages like Modelica [7], [8], which support necessary mathematical descriptions like partial differential equations. Unfortunately, the resulting models are not well suited for MPC due to the complex solution of the resulting optimal control problem (OCP). While it could be solved using evolutionary algorithms, mixed-integer programming has been shown superior for a similar problem [9], [10]. Thus,

the hydrogen's pressure shall be respected in the MPC more implicitly.

One option would be to do so by tracking externally provided setpoints. This is common practice in MPC to optimize objectives which are not (or cannot be) explicitly represented. In this case, the setpoint might be derived from an (arbitrarily complex) heuristic. For example, in [11], a heuristic strategy is used to achieve near-optimal control of direct expansion units of air conditioning systems by adjusting the supply air temperature set-point in dependence of zone conditions and coil status. Note that by providing external (steady-state) setpoints, usually the optimality in regard to the original objectives is lost, which has been the main motivation for the development of economic MPC [12].

In general, the MPC incorporates the model of a system as constraints in the OCP, e.g. ordinary difference equations describing the model dynamics in the form of $x(k+1) = f(x(k), u(k))$ where x is the state vector and u the input vector. However, if a part of the system dynamics is too complex to respect it *explicitly* in this form within the OCP, it is possible to do so *implicitly* by additional constraints. For example, in [13], MPC is used to control the cargo transportation in intermodal hubs. Since the optimization of the transport modal split would be too complex, a heuristic is used. Then, the desired split is incorporated in form of a terminal constraint, which is relaxed to ensure feasibility.

The plant considered in this study has two processes which are too complex to be explicitly considered in an OCP, namely the order in which the 6 MP tanks are fueled and emptied depending on their individual pressure levels, and the *pressure recovery* functionality, which shifts hydrogen between 2 MP sections. Thus, as our main contribution, we propose a novel control strategy to implicitly incorporate these processes. The MPC solves the OCP first neglecting the pressure recovery and individual pressure levels. Then, an alternative (more complex) model is used by the so-called *allocator* to validate whether the MPC's plan is feasible or not, i.e. whether all FCVs can be fueled as planned. If not, the allocator sets additional constraints for the OCP to ensure the fueling success and the MPC runs a second time. Through this approach, we can respect the necessity of sufficiently high storage pressure levels in the fueling process, which is otherwise neglected in the literature. Additionally, we also respect the storage pressure in the calculation of the compressor's mass flow and power consumption while maintaining convexity by piece-wise linear approximations (PWLAs).

The rest of the paper is structured as follows. A more detailed overview of the planned hydrogen system is given in Section II, followed by the description of our proposed control approach in Section III. A simulation study showing its advantages over rule-based controllers is presented in Section IV, followed by a brief discussion and outlook in Section V.

II. SYSTEM OVERVIEW

An overview of the hydrogen plant is depicted in Figure 1. In the following subsections, we give a brief description of the individual entities and how they are modeled in the MPC. We use the standard MPC notation $r(n|k)$, which refers to the value of $r(k+n)$ predicted at time step k . Note that we use varying step sizes $T_s(n|k)$ for different n within the 7-day prediction horizon of the MPC, which has to be respected in the following.

A. Electrolyzer

The core of the plant is a proton exchange membrane (PEM) electrolyzer with a maximum power consumption of $P_{\text{ely,max}} = 225$ kW. It also has a minimum power consumption of $P_{\text{ely,min}} = 70$ kW. Thus, its on/off status has to be considered. Additionally, it has a warm up time of approx. 15 min, which we model by two different binary variables. $b_{\text{ely,on}} \in \{0, 1\}$ denotes the "on" signal sent by the controller, and the auxiliary variable $\tilde{b}_{\text{ely,on}} \in \{0, 1\}$ denotes whether it is ready to produce hydrogen. The power limits are then expressed by

$$\tilde{b}_{\text{ely,on}}(k) \cdot P_{\text{ely,min}} \leq P_{\text{ely}}(k), \quad (1)$$

$$P_{\text{ely}}(k) \leq \tilde{b}_{\text{ely,on}}(k) \cdot P_{\text{ely,max}}. \quad (2)$$

Additionally, $\tilde{b}_{\text{ely,on}}$ is constrained by logical AND conditions [14, §7.7] on the previous values of $b_{\text{ely,on}}$. Due to the varying step sizes, every $\tilde{b}_{\text{ely,on}}(n|k)$ in the horizon may have a different number of constraints. However, to reduce the number of binary decision variables and because later in the horizon, the time steps are bigger than the actual start up constraint time, we do not consider the startup constraints in the entire horizon. The nonlinear mapping of the hydrogen output in dependence of the consumed electrical power, $\dot{m}_{\text{ely}} = f_{\text{ely}}(P_{\text{ely}})$, is formulated as a one-dimensional PWLA [15], which results in additional binary variables and constraints. For this study, we use measurement points taken from [16].

B. Tanks

The LP tank has a maximum capacity of $m_{\text{LP,max}} = 11$ kg at 30 bar and is directly filled by the electrolyzer. The 6 MP tanks have a maximum capacity of ≈ 43.33 kg at 450 bar each. However, due to their complex couplings, they are modelled as a single aggregated tank with $m_{\text{MP,max}} = 260$ kg. Additionally, lower bounds $m_{\text{LP,min}} = 0.5$ kg and $m_{\text{MP,min}} = 60$ kg apply, defined by the constraints

$$m_{\text{LP,min}} \leq m_{\text{LP}}(k) \leq m_{\text{LP,max}}, \quad (3)$$

$$m_{\text{MP,min}} \leq m_{\text{MP}}(k) \leq m_{\text{MP,max}}. \quad (4)$$

The relationship between a tank's pressure and its mass is slightly nonlinear (concave) and temperature dependent. However, for simplicity, in the following we assume $p_{\text{LP}} \propto m_{\text{LP}}$ and $p_{\text{MP}} \propto m_{\text{MP}}$.

The 6 MP tanks are organized in 2 sections with 3 tanks each. The filling of the MP tanks (from the LP tank) is done section-wise. Namely, the section with the higher average pressure

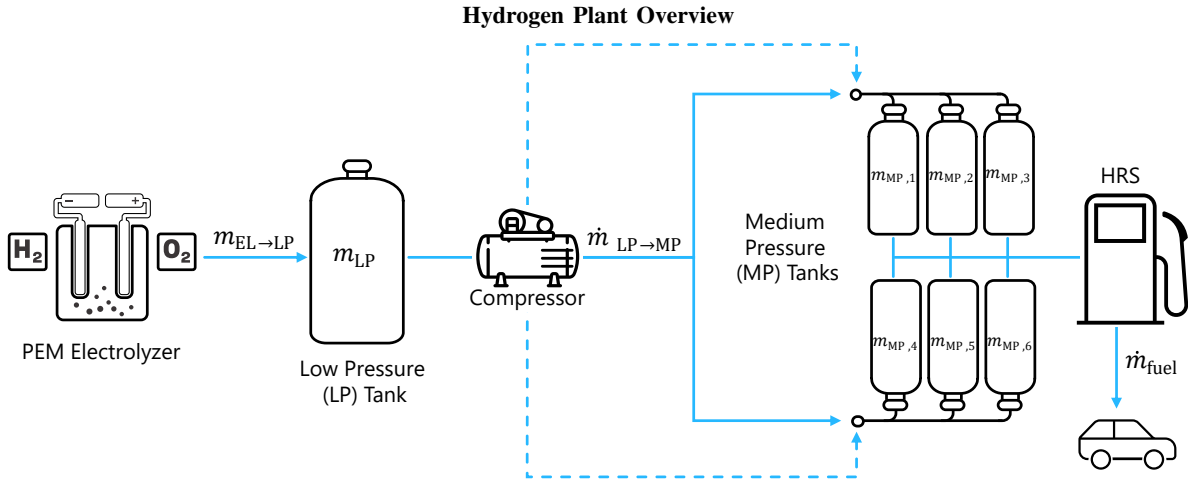


Figure 1: The electrolyzer directly fills the LP tank of max. 11 kg/30 bar capacity. A compressor is then used to transfer the hydrogen to 6 individual MP tanks with max. 43.33 kg/450 bar capacity each, which are organized in 2 sections with 3 tanks each. The compressor can also be used to shift hydrogen between these sections (*pressure recovery*). The HRS (dispenser) is connected to the MP tanks and used to refuel FCVs with 350 bar.

is filled first. Within this section, the tank with the lowest pressure is filled until it has the same pressure as the second lowest tank. Then, these two are filled simultaneously until they have the same pressure as the third, from where on all three are filled simultaneously. When the section hits its upper limit, the other section is being filled according to the same rules.

With the pressure recovery function, hydrogen can also be shifted between the two sections. Thereby, hydrogen is taken from the section with the lower average pressure, and in there from the tank with the lowest pressure, until it hits the lower limit. Then, the next lowest tank (of the same section) is used. The filling of the individual tanks of the other section follows the same rules as described above.

Note that modeling these heuristics explicitly would lead to a non-convex optimization problem. Thus, they are considered implicitly in the proposed allocator approach, see Section III-D.

C. Compressor

The compressor can be used for either transferring hydrogen from the LP tank to the MP tanks, or for the pressure recovery function. Thus, we introduce binary variables for both modes, $b_{comp,LP \rightarrow MP}$ and $b_{comp,PR}$, with the constraint

$$b_{comp,LP \rightarrow MP}(k) + b_{comp,PR}(k) \leq 1. \quad (5)$$

In either case, the compressor's power cannot be modulated. For $b_{comp,LP \rightarrow MP} = 1$, the resulting mass flow $\dot{m}_{LP \rightarrow MP}$ depends on the input pressure, i. e. on m_{LP} . This is respected by a one-dimensional PWLA [15], using the sample points $m_{LP,s} \hat{=} (0, 20, 90)$ bar and $\dot{m}_s^{LP \rightarrow MP} = (0.2, 4.2, 18.0) \frac{\text{kg}}{\text{h}}$. The necessary power $P_{comp,LP \rightarrow MP}$ additionally also significantly depends on the output pressure, i. e. m_{MP} . Thus, a two-dimensional PWLA based on the triangle method is used [15]. For both cases, the resulting constraints are omitted for brevity.

D. Hydrogen Refueling Station (HRS)

For the refueling of FCVs, the uncontrollable demand is modeled as a disturbance $\dot{m}_{fuel,demand}$ in $\frac{\text{kg}}{\text{h}}$. However, the provided hydrogen $\dot{m}_{MP \rightarrow Fuel}$ may deviate, which is expressed as the constraint

$$\dot{m}_{fuel,demand}(k) = \dot{m}_{MP \rightarrow Fuel}(k) + z_{fuel}(k) \quad (6)$$

with a slack variable z_{fuel} , which is punished in the objective function, see (18). The refueling process is done tank-wise, i. e. the MP tank with the lowest possible pressure (i. e. above the car's tank pressure) is always used. Once the MP tank and the car's tank are at the same pressure level, the next higher MP tank is used. To avoid modeling the car tank, we use the MP tank with the lowest pressure above 350 bar.

III. CONTROL APPROACH

To develop the MPC for the above described plant, in this section we first complement its model with the main dynamics, then define objectives to optimize and formulate the resulting OCP. Lastly, we present the novel allocator approach in Section III-D as our main contribution.

A. Plant Model

The discretized tank masses in kg can be described by the ordinary difference equations

$$m_{LP}(k+1) = m_{LP}(k) + (\dot{m}_{ely}(k) - \dot{m}_{LP \rightarrow MP}(k)) \cdot T_s(k), \quad (7)$$

$$m_{MP}(k+1) = m_{MP}(k) + (\dot{m}_{LP \rightarrow MP}(k) - \dot{m}_{MP \rightarrow Fuel}(k)) \cdot T_s(k), \quad (8)$$

where $\dot{m}_{LP \rightarrow MP}$ is the compressor's and $\dot{m}_{MP \rightarrow Fuel}$ the HRS's mass flow in $\frac{\text{kg}}{\text{h}}$.

The electrical balance equation is given by

$$0 = P_{\text{grid}}(k) + P_{\text{dem}}(k) + P_{\text{PV}}(k) - P_{\text{ely}}(k) - b_{\text{comp,L P} \rightarrow \text{MP}}(k) \cdot P_{\text{comp,L P} \rightarrow \text{MP}}(k) - b_{\text{comp,PR}}(k) \cdot P_{\text{comp,PR}}, \quad (9)$$

where we assume a constant value for $P_{\text{comp,PR}}$.

B. Objectives

1) *Soft Constraints on Tank Limits:* For both the LP and MP tanks, increased lower limits ($m_{\text{LP,min}}^{\text{soft}} = 7 \text{ kg} > m_{\text{LP,min}}$, $m_{\text{MP,min}}^{\text{soft}} = 151.9 \text{ kg} > m_{\text{MP,min}}$) are enforced using soft constraints. Instead of a relaxed version of constraints (3) and (4), we introduce the objective costs

$$J_{\text{SC,LP}}(k) = 0.1 \cdot \sum_{n=0}^{N_p} \max(0, m_{\text{LP,min}}^{\text{soft}} - m_{\text{LP}}(n|k)) \cdot T_s(n|k), \quad (10)$$

$$J_{\text{SC,MP}}(k) = 0.1 \cdot \sum_{n=0}^{N_p} \max(0, m_{\text{MP,min}}^{\text{soft}} - m_{\text{MP}}(n|k)) \cdot T_s(n|k). \quad (11)$$

$m_{\text{LP,min}}^{\text{soft}}$ is chosen such that an input pressure of at least 20 bar for the compressor is ensured. $m_{\text{MP,min}}^{\text{soft}}$ is chosen such that there is enough hydrogen to have one section (i.e. 3 tanks) above 350 bar, plus additional 4 kg hydrogen to refuel a car at any time.

2) *Monetary Costs:* For the grid costs, different prices $c_{\text{grid,buy}} = 0.144 \text{ €/kWh}$ for buying and $c_{\text{grid,sell}} = 0.07 \text{ €/kWh}$ for selling are assumed. To formulate them not only convexly, but also following disciplined parametrized programming (DPP)¹ rules, we use an auxiliary parameter $c_{\text{grid,diff}} = c_{\text{grid,buy}} - c_{\text{grid,sell}} > 0$, with which the costs are described as

$$J_{\text{mon}}^{\text{grid}}(k) = \sum_{n=0}^{N_p-1} (c_{\text{grid,diff}}(n|k) \cdot \max(0, P_{\text{grid}}(n|k)) + c_{\text{grid,sell}}(n|k) \cdot P_{\text{grid}}(n|k)) \cdot T_s(n|k). \quad (12)$$

Additionally, a penalty for the highest power peak has to be paid, as is common in German industry pricing. It can be expressed as [17], [18]

$$\tilde{c}_{\text{peak}}^{\text{max}}(n|k) = c_{\text{grid,peak}} \cdot P_{\text{grid}}(n|k) - J_{\text{mon,peak}}^{\text{previous}}(k) \quad (13)$$

$$J_{\text{mon}}^{\text{peak}}(k) = \max_{n=0, \dots, N_p-1} (\max(0, \tilde{c}_{\text{peak}}^{\text{max}}(n|k))), \quad (14)$$

with $c_{\text{grid,peak}} = 122.07 \text{ €/kW}$. $J_{\text{mon,peak}}^{\text{previous}}$ is implemented as a parameter which is calculated before each time step and denotes the already occurred peak costs.

The total monetary costs are then

$$J_{\text{mon,total}}(k) = J_{\text{mon}}^{\text{grid}}(k) + J_{\text{mon}}^{\text{peak}}(k). \quad (15)$$

¹See <https://www.cvxpy.org/tutorial/advanced/index.html#disciplined-parametrized-programming>

3) *Operational Costs:* Frequent startups increase an electrolyzer's degradation. Thus, we punish every startup of the electrolyzer by

$$\delta_{\text{on-off}}(k) = b_{\text{ely,on}}(k) - b_{\text{ely,on}}(k-1), \quad (16)$$

$$J_{\text{startup}}(k) = \sum_{n=0}^{N_p-1} \max(0, c_{\text{startup}} \cdot \delta_{\text{on-off}}(n|k)) \quad (17)$$

with $c_{\text{startup}} = 10$.

4) *User Satisfaction:* To enforce that any fuel demand is satisfied as much as possible, we punish the mismatch slack variable z_{fuel} from (6) strongly, i.e.

$$J_{\text{user}}(k) = c_{\text{fueldemand}}^{\text{mismatch}} \sum_{n=0}^{N_p-1} z_{\text{fuel}}(n|k) \cdot T_s(n|k), \quad (18)$$

with $c_{\text{fueldemand}}^{\text{mismatch}} = 200 \text{ €/kg}$.

5) *CO₂ Emissions:* We punish CO₂ emissions separately, i.e.

$$J_{\text{CO}_2}(k) = \sum_{n=0}^{N_p-1} c_{\text{grid,CO}_2} \cdot \max(0, P_{\text{grid}}(n|k)) \cdot T_s(n|k), \quad (19)$$

with $c_{\text{grid,CO}_2} = 0.02 \text{ €/kWh}$.

C. Optimal Control Problem (OCP)

The objective function of the OCP is the sum of all costs described above, i.e.

$$J_{\text{total}}(k) = J_{\text{SC,LP}}(k) + J_{\text{SC,MP}}(k) + J_{\text{mon}}^{\text{grid}}(k) + J_{\text{mon}}^{\text{peak}}(k) + J_{\text{startup}}(k) + J_{\text{user}}(k) + J_{\text{CO}_2}(k). \quad (20)$$

Note that various approaches exist to derive appropriate weights for the individual objectives, if user preferences should be respected [19], [20]. The decision variables are the actual inputs, $u = (P_{\text{ely}}, b_{\text{ely,on}}, b_{\text{comp,L P} \rightarrow \text{MP}}, b_{\text{comp,PR}}, \dot{m}_{\text{MP} \rightarrow \text{Fuel}}, P_{\text{grid}})$ as well as the auxiliary variables $u_{\text{aux}} = (\tilde{b}_{\text{ely,on}}, z_{\text{fuel}}, \dots)$ with all the additional variables from the PWLA formulations and logical AND conditions. Let u and u_{aux} denote the sequences of these vectors, e.g. $u(k) = (u(0|k), \dots, u(N_{\text{pred}}-1|k))$. The prediction horizon is 7 days long and split into $N_{\text{pred}} = 35$ unequal steps, i.e.

$$T_s = (5 \text{ min}, 10 \text{ min}, 15 \text{ min}, 3 * 30 \text{ min}, 22 * 1 \text{ h}, 2 * 12 \text{ h}, 5 * 24 \text{ h}),$$

where $a * b$ denotes a steps of length b . Then, the OCP is given by

$$\min_{u, u_{\text{aux}}} J_{\text{total}}(k) \quad (21)$$

s. t. (5), (6), (7), (8), (9) $\forall n = 0 \dots N_{\text{pred}} - 1$

(3), (4), $\forall n = 1 \dots N_{\text{pred}}$,

constr. by 1DPWLAs on $\dot{m}_{\text{ely}}(P_{\text{ely}}), \dot{m}_{\text{LP} \rightarrow \text{MP}}(m_{\text{LP}})$,

constr. by 2DPWLA on $P_{\text{comp,L P} \rightarrow \text{MP}}(m_{\text{LP}}, m_{\text{MP}})$,

constr. by AND conditions on $\tilde{b}_{\text{ely,on}}$ & $b_{\text{ely,on}}$,

where the time step notation (k) and ($k+1$) in (3)–(9) are to be read as ($n|k$) and ($n+1|k$), respectively.

D. Allocator

The MPC is unaware of the individual MP tanks' pressure levels. However, for the HRS, it is crucial whether at least a single MP tank has enough pressure to fuel a car. Thus, in this paragraph we present the proposed allocator approach. Figure 2 gives an overview of the entire simulation flow. Algorithm 1 describes the differences in the iteration of the heuristic simulation model to the MPC's internal model. Algorithm 2 describes how the allocator determines whether additional constraints on the OCP are necessary.

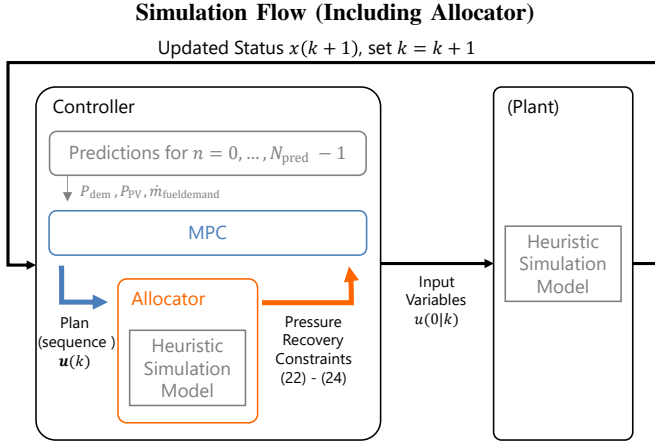


Figure 2: The allocator uses a second, heuristic simulation model, which models all 6 MP tanks individually. Using the input variables determined by the MPC solving (21), it checks whether all planned car refueling events would be successful, i.e. if at least one tank with enough pressure is present. If not, it sets the parameters for the constraints (22)–(24) and the MPC runs a second time. Afterwards, the first input variables of the updated plan are sent to the plant. In this work, we use the same heuristic simulation model as in the allocator as the plant. Finally, the state is updated and the entire process repeated for the next time step.

The allocator sets constraints on the PR only in the first 8 h of the horizon, which corresponds to the first $n_{\text{cutoff}} = 12$ steps,

$$\sum_{k=0}^{n_{\text{cutoff}}-1} b_{\text{considerPR}}(k) \cdot b_{\text{comp,PR}}(k) \cdot T_s(k) \geq t_{\text{PR}}, \quad (22)$$

$$b_{\text{considerPR}}(k) = 0 \quad \forall k = n_{\text{cutoff}} \dots N_{\text{pred}} - 1, \quad (23)$$

where $t_{\text{PR}} \geq 0$ in hours defines how long the PR should run. Additionally, a higher limit on m_{MP} may be set to ensure that enough hydrogen is available to be shifted between the sections,

$$m_{\text{MP}}(k) \geq m_{\text{MP,lim}}^{\text{alloc}}(k) - z_{\text{lim,alloc}}(k) \quad \forall k = 0 \dots n_{\text{cutoff}} - 1. \quad (24)$$

$z_{\text{lim,alloc}}$ is used to soften the constraint in combination with a cost function analogous to (10) with a weight of 1. If constraints on t_{PR} and $b_{\text{considerPR}}$ or on $m_{\text{MP,lim}}^{\text{alloc}}$ are set, the MPC resolves the OCP (21) including the new constraints.

IV. SIMULATION STUDY

To evaluate the proposed control approach, we performed a simulation study, where we simulated the controller against

Algorithm 1: Excerpt of the heuristic simulation model's iteration. Parts which are identical with the MPC's internal model are omitted.

Inputs: Decision variables u , all tank masses, T_s
 $h =$ section with higher mass, $\ell =$ section with lower mass;

```

// Do Pressure Recovery
if  $b_{\text{comp,PR}} = 1$  and  $m_{\text{MP,sec,1}} \neq m_{\text{MP,sec,2}}$  then
     $m_{\text{PR,plan}} = \dot{m}_{\text{PR,nominal}} \cdot T_s$ ;
    Determine tank order (ascending masses) in lower
    section:  $\ell_1, \ell_2, \ell_3$ ;
     $m_{\text{PR,available}} =$  Available hydrogen available for
    PR (before either lower or higher limit of
    tanks/sections is hit);
     $m_{\text{PR,to move}} = \min(m_{\text{PR,plan}}, m_{\text{PR,available}})$ ;
    for  $i$  in  $\{\ell_1, \ell_2, \ell_3\}$  do
         $m_{\text{PR,temp}} =$ 
             $\min(m_{\text{PR,to move}}, m_{\text{MP},i} - m_{\text{MP},i,\text{min}})$ ;
        // Fill section  $h$  with  $m_{\text{PR,temp}}$ 
         $m_{\text{filled}} = \text{fill\_section}(h, m_{\text{PR,temp}})$ ;
         $m_{\text{MP},i} -= m_{\text{filled}}$ ;
         $m_{\text{PR,to move}} -= m_{\text{filled}}$ ;
        if  $m_{\text{PR,temp}} = 0$  then
            | Break
        end
    end
end

// Do HRS Refueling
 $m_{\text{to fuel}} = \dot{m}_{\text{MP} \rightarrow \text{Fuel}} \cdot T_s$ ;
 $\dot{m}_{\text{fuel,real}} = 0$ ;
if  $m_{\text{to fuel}} > 0$  then
    Determine fuel_order, i.e. tanks with ascending
    masses;
    for  $i$  in fuel_order do
         $\dot{m}_{\text{fuel,use},i} = \min(m_{\text{to fuel}}, m_{\text{MP},i} - m_{\text{MP},i}(p =$ 
             $350 \text{ bar}), 0)$ ;
         $m_{\text{to fuel}} -= \dot{m}_{\text{fuel,use},i}$ ;
         $m_{\text{MP},i} -= \dot{m}_{\text{fuel,use},i}$ ;
         $\dot{m}_{\text{fuel,real}} += \dot{m}_{\text{fuel,use},i} / T_s$ ;
        if  $m_{\text{to fuel}} = 0$  then
            | Break
        end
    end
end

// Do Filling LP -> MP
 $m_{\text{to fill}} = \dot{m}_{\text{LP} \rightarrow \text{MP}} \cdot T_s$ ;
if  $m_{\text{to fill}} > 0$  then
     $m_{\text{filled},h} = \text{fill\_section}(h, m_{\text{to fill}})$ ;
     $m_{\text{to fill}} -= m_{\text{filled},h}$ ;
end
if  $m_{\text{to fill}} > 0$  then
     $m_{\text{filled},\ell} = \text{fill\_section}(\ell, m_{\text{to fill}})$ ;
     $m_{\text{to fill}} -= m_{\text{filled},\ell}$ ;
end

```

Algorithm 2: Allocator logic to determine additional constraints on pressure recovery (PR) and m_{MP} .

Inputs: $u(k)$

Outputs: $b_{\text{considerPR}}(k)$, $t_{\text{PR}}(k)$, $m_{\text{MP,lim}}^{\text{alloc}}(k)$

Get state sequence x and adjusted input sequence u_{adj} from heuristic simulation model (see Algorithm 1);

Calculate (unplanned) mismatches $\dot{m}_{\text{fuel,mismatch}}$ between $\dot{m}_{\text{MP} \rightarrow \text{Fuel}}$ from u and u_{adj} ;

if $\sum_n \dot{m}_{\text{fuel,mismatch}}(n|k) > 0$ **then**
 Determine first step n_{fm} in prediction horizon for which $\dot{m}_{\text{fuel,mismatch}}(n_{\text{fm}}|k) > 0$;

Determine how much hydrogen $m_{\text{available for PR}}$ would be available for PR at this time;

if $n_{\text{fm}} \leq n_{\text{cutoff}}$ **AND** $m_{\text{available for PR}}(n_{\text{fm}}|k) > 0$ **then**

$b_{\text{considerPR}}(n) \leftarrow 1 \quad \forall n = 0, \dots, n_{\text{fm}} - 1$

Determine $m_{\text{move with PR}}$ as minimum of $m_{\text{available for PR}}(n_{\text{fm}}|k)$ and necessary amount to have higher section at 350 bar + fuel demand;

$t_{\text{PR}} = m_{\text{move with PR}} / \dot{m}_{\text{PR,nominal}}$;

$t_{\text{PR}} \leftarrow \min(t_{\text{PR}}, \sum_{n=0}^{n_{\text{fm}}} T_s(n))$;

end

Determine possible upper limits $m_{\text{MP,possible}}$ with maximum hydrogen production;

$m_{\text{MP,350 bar limit}}$ = lower limit to have at least one section with 350 bar;

for every n **with** $\dot{m}_{\text{fuel,mismatch}}(n|k) > 0$ **do**

$m_{\text{MP,lim}}^{\text{alloc}}(n|k) \leftarrow$

$\min(m_{\text{MP,possible}}(n|k), m_{\text{MP,350 bar limit}} + \dot{m}_{\text{MP} \rightarrow \text{Fuel}}(n|k) \cdot T_s(n))$;

end

end

the heuristic model used in the allocator, as proposed in Section III-D. This is illustrated in Figure 2.

In the first subsection, we briefly describe the simulation setup. To benchmark the proposed approach, we compare it to two rule-based control strategies which are described in Section IV-B. Finally, we discuss the results of the study in Section IV-C.

A. Setup

For the simulation, real measurement data of the Honda Europe R&D facility in Offenbach, Germany was used for the load demand and PV power. The hydrogen demand profile for the HRS was generated using a statistical usage scenario: We generate a set of N_{sessions} random FCV fueling sessions for each calendar week of the year, where $N_{\text{sessions}} \sim \mathcal{U}[5, 10]$. FCVs arrive with equal probability on Monday – Friday, while no cars arrive on weekends. For each session, we draw an arrival time t_{arrival} and a hydrogen demand m_{H_2} . 50% of the sessions occur between 7 – 9:30 a.m., with 10% between 12 – 1 p.m., and 40% between 4:30 – 6:30 p.m. Therefore, a time window

for t_{arrival} is selected accordingly. Within the selected window, t_{arrival} is distributed uniformly. The demand is sampled as $m_{\text{H}_2} = \max(4 \text{ kg}, \tilde{m}_{\text{H}_2})$, with $\tilde{m}_{\text{H}_2} \sim \mathcal{N}(3 \text{ kg}, (0.5 \text{ kg})^2)$. Each fueling session is assumed to take 5 min and the fuel demand rate $\dot{m}_{\text{fuel,demand}}$ is calculated accordingly. In total, 410 fueling sessions were generated for the simulated year. The process of generating sessions was adapted from [21].

As initial states of the tanks, we assume $m_{\text{LP}}(0) = 5 \text{ kg}$, $m_{\text{MP},1}(0) = 83 \text{ kg}$, $m_{\text{MP},2}(0) = 82 \text{ kg}$, $m_{\text{MP},3}(0) = 81 \text{ kg}$, $m_{\text{MP},4}(0) = 80 \text{ kg}$, $m_{\text{MP},5}(0) = 60 \text{ kg}$, $m_{\text{MP},6}(0) = 60 \text{ kg}$. Furthermore, the initial peak limit is $P_{\text{grid,peak}}(0) = 500 \text{ kW}$ and the electrolyzer is off, i. e. $b_{\text{ely,on}}(0) = 0$.

We simulated the full calendar year of 2021 using perfect predictions. An analysis of the influence of prediction errors for the photovoltaic (PV) power output on the peak costs can be found in [22]. The controller, model and simulation framework were implemented in Python, using CVXPY [23] to model the OCP and to interface Gurobi [24] as the solver. The simulation step size is $T_s(0|k) = 5 \text{ min}$. We simulated on an Intel i5-9400, with a solver time limit of 20s and an optimality gap of 10^{-4} . The MPC simulation took approx. 11 h, and the rule-based controller simulations approx. 12 min each.

B. Rule-Based Benchmark Controllers

To benchmark the performance of the proposed approach, we propose two baseline rule-based controllers. The first controller (RBC Peak) uses as much power as is available without causing a new peak to operate the electrolyzer, i. e.

$$P_{\text{available}}^{\text{Peak}}(k) = \max(P_{\text{grid,peak}}(k) + P_{\text{PV}}(k) + P_{\text{dem}}(k) - P_{\text{comp,max}}, 0). \quad (25)$$

The second controller (RBC Excess) uses only available excess PV power, i. e.

$$P_{\text{available}}^{\text{Excess}}(k) = \max(0, P_{\text{PV}}(k) + P_{\text{dem}}(k)). \quad (26)$$

Both controllers employ the same logic to apply $P_{\text{available}}(k)$ to operate the plant. This logic is illustrated in Algorithm 3. Note that the RBC Excess controller may also use non-PV excess power to run the compressor or perform pressure recovery. As for the MPC, $T_s = 5 \text{ min}$ is used for both controllers.

C. Simulation Results

Table I shows the results of the simulation study in terms of yearly key performance indicators (KPIs). The electricity costs do not contain the peak costs. The PV self consumption rate is defined as the fraction of PV energy that is not fed back into the grid. The costs per kg of hydrogen are calculated from the electricity costs incurred by the operation of any of the hydrogen components (i. e. electrolyzer, compressor). Here, the energy that could be covered with PV excess is accounted for with the feed-in tariff $c_{\text{grid,sell}}$, and power from grid with the grid tariff $c_{\text{grid,buy}}$. The fueling success rate is the fraction of fulfilled hydrogen demand and total hydrogen demand.

Algorithm 3: Operational logic of rule-based controllers

```

 $m_{\text{ely,min}}(k) = \dot{m}_{\text{ely}}(P_{\text{ely,min}}) \cdot T_s;$ 
 $m_{\text{ely,max}}(k) = m_{\text{LP,max}} - m_{\text{LP}}(k);$ 
if  $P_{\text{available}}(k) \geq P_{\text{ely,min}}$  AND  $m_{\text{ely,max}}(k) \geq$ 
 $m_{\text{ely,min}}(k)$  then
   $b_{\text{ely,on}}(k) \leftarrow 1;$ 
  if  $b_{\text{ely,ready}}^{\text{measured}}(k) = 1$  then
     $P_{\text{max}}(k) =$ 
     $\max(P_{\text{ely}}(m_{\text{ely,max}}(k)/T_s), P_{\text{ely,max}});$ 
     $P_{\text{ely}}(k) \leftarrow \min(P_{\text{available}}(k), P_{\text{max}}(k));$ 
  else
     $P_{\text{ely}}(k) \leftarrow 0$ 
  end
end
 $P_{\text{res}}(k) = P_{\text{available}}(k) - P_{\text{ely}}(k);$ 
if  $P_{\text{dem}}(k) - P_{\text{comp,max}} + P_{\text{res}}(k) \leq P_{\text{grid,peak}}(k)$  then
  if Transfer from LP → MP possible then
     $b_{\text{comp,LP→MP}}(k) \leftarrow 1$ 
  else
     $b_{\text{comp,PR}}(k) \leftarrow 1$ 
  end
end
 $\dot{m}_{\text{MP→Fuel}}(k) \leftarrow \dot{m}_{\text{fueldemand}}(k)$ 

```

The results in Table I show that the RBC Excess controller incurs the lowest electricity costs at the highest PV self consumption rate. As the controller uses mostly excess PV power, it naturally incurs the lowest costs of hydrogen production and lowest CO₂ emissions. Yet, this comes at the cost of the fueling success rate being very low. This is due to the total amount of hydrogen produced being half of what the RBC Peak or MPC controllers produce, indicating that for the given plant, excess PV power is not sufficient to fulfill hydrogen demand. This is further illustrated in Figure 3. The figure shows the costs per kg hydrogen, fuel success rate and PV self consumption in each month of the simulated year. In the winter months, the comparatively low amount of available PV energy is not enough to fulfill the hydrogen demand, indicated by the very low fuel success rate of the RBC Excess controller.

Compared to the RBC Peak controller, the proposed MPC approach incurs lower electricity costs while also producing hydrogen at a significantly lower cost. The hydrogen production costs of the MPC are only slightly higher than those of the RBC Excess controller, while achieving a significantly higher fuel success rate of 100%. The RBC Peak controller produces approx. 90 kg hydrogen more than the MPC at a lower overall PV self consumption rate. Furthermore, the RBC Peak controller produces 49 more startups of the electrolyzer compared to the MPC. While the average number of startups per day is still less than 1, the total number of startups should be minimized, as these degrade the hydrogen stacks.

The RBC Peak controller exhibits a decreased fuel success rate in January, as can be seen in the middle plot of Figure 3.

This is due to the initial tank conditions. The rule-based controllers only perform pressure recovery if no electrolyzer operation is possible and/or no peak power demand would be caused. In January, this behavior in combination with the initial conditions causes the RBC Peak controller to not perform pressure recovery in the beginning of the month, whereby the demand of the first two cars arriving cannot be fulfilled completely.

Table I: KPIs of the proposed control approaches for the year 2021.

KPI	MPC	RBC Excess	RBC Peak
Electricity costs in 1000 Euro	249.43	244.45	253.25
Max. peak in kW	544.88	544.88	544.88
CO ₂ emissions in kg	760.57	735.87	773.58
Produced H ₂ in kg	1245.77	752.36	1336.01
Elect. costs per kg H ₂ in Euro	9.17	8.54	11.41
Fueling success rate in %	100.00	54.49	99.58
PV self consumption in %	86.42	93.41	85.24
PV self consumption in MWh	587.38	634.85	579.34
Number of electrolyzer startups	297	289	348

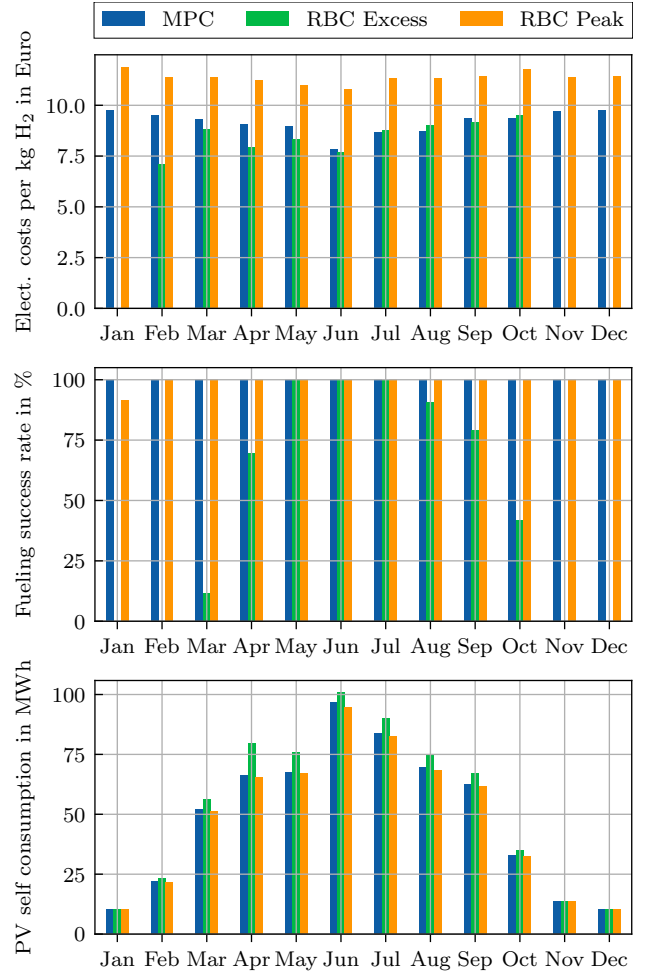


Figure 3: Electricity costs per kg hydrogen, fueling success rate and PV self consumption in each month of the simulated year 2021 for the proposed MPC approach, the RBC Excess controller and the RBC Peak controller.

V. CONCLUSION

We proposed an MPC approach with implicit incorporation of heuristics for the operation of a hydrogen plant. From the overall results of the simulation study, we conclude that the proposed approach operates the plant effectively and efficiently. Furthermore, we have shown that it outperforms the two proposed rule-based benchmark controllers.

While the simulation study showcases the efficacy of the proposed MPC approach, this should be validated on the actual hardware of the hydrogen plant. As an intermediate step, the approach could be validated through software-in-the-loop (SiL) simulation using a high-fidelity digital twin of the facility, as was done in [25]. Thus, future work will involve the implementation and testing of the proposed MPC controller in SiL simulation on a digital twin and on the physical plant.

REFERENCES

- [1] M. İnci, M. Büyüç, M. H. Demir, and G. İlbey, "A review and research on fuel cell electric vehicles: Topologies, power electronic converters, energy management methods, technical challenges, marketing and future aspects," *Renewable and Sustainable Energy Reviews*, vol. 137, p. 110648, 2021. [Online]. Available: <https://www.sciencedirect.com/science/article/pii/S1364032120309321>
- [2] R. C. Samsun, M. Rex, L. Antoni, and D. Stolten, "Deployment of fuel cell vehicles and hydrogen refueling station infrastructure: a global overview and perspectives," *Energies*, vol. 15, no. 14, p. 4975, 2022.
- [3] M. Stadie, T. Rodemann, A. Burger, F. Jomrich, S. Limmer, S. Rebhan, and H. Saeki, "V2b vehicle to building charging manager," in *Proceedings of the EVTeC: 5th International Electric Vehicle Technology Conference*, 2021. [Online]. Available: <https://www.honda-ri.de/pubs/pdf/4658.pdf>
- [4] C. Huang, Y. Zong, S. You, C. Tröholt, Y. Zheng, J. Wang, Z. Zheng, and X. Xiao, "Economic and resilient operation of hydrogen-based microgrids: An improved MPC-based optimal scheduling scheme considering security constraints of hydrogen facilities," *Applied Energy*, vol. 335, p. 120762, 2023. [Online]. Available: <https://www.sciencedirect.com/science/article/pii/S0306261923001265>
- [5] P. Cardona, R. Costa-Castelló, V. Roda, J. Carroquino, L. Valiño, and M. Serra, "Model predictive control of an on-site green hydrogen production and refuelling station," *International Journal of Hydrogen Energy*, 2023. [Online]. Available: <https://www.sciencedirect.com/science/article/pii/S036031992300383X>
- [6] M. B. Abdelghany, M. F. Shehzad, V. Mariani, D. Liuzza, and L. Glielmo, "Two-stage model predictive control for a hydrogen-based storage system paired to a wind farm towards green hydrogen production for fuel cell electric vehicles," *International Journal of Hydrogen Energy*, vol. 47, no. 75, pp. 32 202–32 222, 2022. [Online]. Available: <https://www.sciencedirect.com/science/article/pii/S0360319922031871>
- [7] T. Kuroki, N. Sakoda, K. Shinzato, M. Monde, and Y. Takata, "Dynamic simulation for optimal hydrogen refueling method to fuel cell vehicle tanks," *International Journal of Hydrogen Energy*, vol. 43, no. 11, pp. 5714–5721, 2018. [Online]. Available: <https://www.sciencedirect.com/science/article/pii/S0360319918302234>
- [8] E. Rothuizen, W. Mérida, M. Rokni, and M. Wistoft-Ibsen, "Optimization of hydrogen vehicle refueling via dynamic simulation," *International Journal of Hydrogen Energy*, vol. 38, no. 11, pp. 4221–4231, 2013. [Online]. Available: <https://www.sciencedirect.com/science/article/pii/S036031991300270X>
- [9] H. K. Singh, T. Ray, M. J. Rana, S. Limmer, T. Rodemann, and M. Olhofer, "Investigating the use of linear programming and evolutionary algorithms for multi-objective electric vehicle charging problem," *IEEE Access*, vol. 10, pp. 115 322–115 337, 2022.
- [10] T. Ishihara and S. Limmer, "Optimizing the hyperparameters of a mixed integer linear programming solver to speed up electric vehicle charging control," in *Applications of Evolutionary Computation: 23rd European Conference, EvoApplications 2020, Held as Part of EvoStar 2020, Seville, Spain, April 15–17, 2020, Proceedings 23*. Springer, 2020, pp. 37–53.
- [11] J. Cai and J. E. Braun, "A generalized control heuristic and simplified model predictive control strategy for direct-expansion air-conditioning systems," *Science and Technology for the Built Environment*, vol. 21, no. 6, pp. 773–788, 2015. [Online]. Available: <https://doi.org/10.1080/23744731.2015.1040327>
- [12] R. Amrit, J. B. Rawlings, and D. Angeli, "Economic optimization using model predictive control with a terminal cost," *Annual Reviews in Control*, vol. 35, no. 2, pp. 178–186, 2011.
- [13] J. L. Nabais, R. R. Negenborn, R. B. C. Benítez, and M. A. Botto, "A constrained MPC heuristic to achieve a desired transport modal split at intermodal hubs," in *16th International IEEE Conference on Intelligent Transportation Systems (ITSC 2013)*. IEEE, 2013, pp. 714–719.
- [14] J. Bisschop, *AIMMS optimization modeling*. Lulu Press, 2006. [Online]. Available: http://download.aimms.com/aimms/download/manuals/AIMMS3_OM.pdf
- [15] C. D'Ambrosio, A. Lodi, and S. Martello, "Piecewise linear approximation of functions of two variables in MILP models," *Operations Research Letters*, vol. 38, no. 1, pp. 39–46, 2010.
- [16] M. Kopp, *Strommarktseitige Optimierung des Betriebs einer PEM-Elektrolyseanlage*. kassel university press GmbH, 2018.
- [17] T. Schmitt, T. Rodemann, and J. Adamy, "Multi-objective model predictive control for microgrids," *at - Automatisierungstechnik*, vol. 68, no. 8, pp. 687 – 702, 2020. [Online]. Available: <https://www.honda-ri.de/pubs/pdf/4361.pdf>
- [18] T. Schmitt, "Multi-objective building energy management optimization with model predictive control," Ph.D. dissertation, Technische Universität Darmstadt, Darmstadt, 2022. [Online]. Available: <http://tuprints.ulb.tu-darmstadt.de/22344/>
- [19] T. Schmitt, M. Hoffmann, T. Rodemann, and J. Adamy, "Incorporating human preferences in decision making for dynamic multi-objective optimization in Model Predictive Control," *Inventions*, vol. 7, no. 3, 2022. [Online]. Available: <https://www.mdpi.com/2411-5134/7/3/46>
- [20] T. Schmitt, J. Engel, T. Rodemann, and J. Adamy, "Application of Pareto optimization in an economic model predictive controlled microgrid," in *2020 28th Mediterranean Conference on Control and Automation (MED)*. IEEE, 2020, pp. 868–874. [Online]. Available: <https://www.honda-ri.de/pubs/pdf/4341.pdf>
- [21] J. Engel, T. Schmitt, T. Rodemann, and J. Adamy, "Hierarchical economic model predictive control approach for a building energy management system with scenario-driven EV charging," *IEEE Transactions on Smart Grid*, pp. 1–1, 2022.
- [22] T. Schmitt, T. Rodemann, and J. Adamy, "The cost of photovoltaic forecasting errors in microgrid control with peak pricing," *Energies*, vol. 14, no. 9, 2021. [Online]. Available: <https://www.mdpi.com/1996-1073/14/9/2569>
- [23] S. Diamond and S. Boyd, "CVXPY: A Python-embedded modeling language for convex optimization," *Journal of Machine Learning Research*, vol. 17, no. 83, pp. 1–5, 2016.
- [24] Gurobi Optimization, LLC, "Gurobi Optimizer Reference Manual," 2023. [Online]. Available: <https://www.gurobi.com>
- [25] T. Schmitt, J. Engel, and T. Rodemann, "Regression-based model error compensation for a hierarchical MPC building energy management system," in *2023 IEEE Conference on Control Technology and Applications (CCTA)*, 2023, accepted (preprint available at <https://arxiv.org/abs/2306.09080>).